River Flow 2010 - Dittrich, Koll, Aberle & Geisenhainer (eds) - © 2010 Bundesanstalt für Wasserbau ISBN 978-3-939230-00-7

Turbulent Flow in the Scour Hole Downstream of a Sluice Gate: Erosion induced by Görtler Vortices

B. Rodriguez & C. Escauriaza
Hydraulic and Environmental Engineering Department, Pontificia Universidad Católica de Chile, Santiago, Chile

ABSTRACT: Erosion and sediment transport processes in rivers and channels usually take place in arbitrary geometries and occur in turbulent conditions at high Reynolds numbers. Coherent structures that emerge from large-scale instabilities can play a fundamental role in sediment transport, and in many cases they constitute the most important mechanism of bed-load transport and scour in non-equilibrium conditions. The recent experiments carried out by Hopfinger et al. (J. Fluid Mech. 520, 2004) and Albayrak et al. (J. Fluid Mech. 606, 2008) have shown that streamwise Görtler vortices have a considerable impact on sediment transport rates and scour produced by a wall-jet flow downstream of a sluice gate. Görtler vortices emerge in an advanced stage of scour due to the concave curvature of the bed inside the scour hole and their interaction with the bed increases the shear stress and intensifies bed-load transport. To understand better the relation between coherent structures and sediment transport, we carry out detached-eddy simulations (DES) of the flow studied by Albayrak et al. (2008). We reproduce the original experimental configuration, by discretizing the domain using body-fitted curvilinear grid with a total of 9.7 million nodes. Our simulations can resolve the coherent structures of the flow at Re = 156,200, and capture the dynamics of the Görtler vortices inside the scour hole. The model not only reproduces the unsteady flowfield, but also the dynamic features of the shear-stress induced by the Görtler vortices, which are responsible for the sediment streaks that appear on the bed. The model can therefore serve as a powerful tool to predict sediment transport and scour under non-equilibrium conditions.

Keywords: Turbulent flows, Computational fluid dynamics (CFD), Görtler vortices, Scour, Sediment transport.

1 INTRODUCTION

Turbulent flows in fluvial systems usually take place in arbitrarily complex topographies. They are also highly three-dimensional, and characterized by a wide range vortical scales that dominate sediment transport and erosion processes. These flows are further complicated when they interact with hydraulic structures, which produce unsteady vortices that emerge from flow instabilities, increasing the stresses on the bed and initiating local scour.

These characteristics present a great challenge to numerical models intended to study the effects of unsteady coherent structures in sediment transport problems. At engineering scales, unsteady Reynolds-averaged Navier Stokes (URANS) models are usually employed to compute the mean flowfield, and account for the effects of the turbulence fluctuations by using a gradient-diffusion hypothesis to estimate the eddy-viscosity from transport equations. Recent investigations (Paik et al., 2007; Escauriaza and Sotiropoulos, 2010) have demonstrated that URANS models fail to capture the unsteady features of flows driven by dynamically-rich coherent structures, such as the horseshoe vortex system around obstacles mounted on the bed (Escauriaza and Sotiropoulos, 2010). On the other hand, large-eddy simulations (LES) models can resolve the most important vortical structures in the flow, but they might become computationally expensive in complex flows at high Reynolds numbers in engineering applications. Recently, hybrid models such as detached eddy simulations (DES) have shown to be powerful tools to resolve the large-scale coherent structures with moderate computational resources (Spalart et al., 1997; Spalart, 2009). DES com-

bines the advantages of both, URANS and LES strategies, employing URANS models near solid walls, and LES in the rest of domain.

Clear examples on the importance of coherent structures arising from large-scales instabilities of the mean flow are the studies of Hopfinger et al. (2004) and Albayrak et al. (2008). These authors studied experimentally the scour produced by a wall-jet downstream of a sluice gate, and observed that the development of a concave bed surface due to initial scour triggered a centrifugal instability, producing counter-rotating streamwise pairs of Görtler vortices inside the scour hole. These vortices played a significant role in the continuous development of scour as they generated high turbulent stresses and increased considerably the total sediment flux. Albayrak et al. (2008) performed statistical analyses of flow variables on flat and concave walls, and observed experimentally for the second case the dynamic manifestation of streamwise Görtler vortices with a 3D acoustic profiler (ADVP).

Görtler vortices emerge by the instability of the turbulent boundary layer and the bed curvature inside the scour hole (Saric, 1994). This phenomenon arises as a consequence of the bed curvature and a velocity profile that decreases its magnitude with radius of curvature. Several flows in these conditions have been thoroughly studied, such as Blasius velocity profiles or wall-jet profiles (Floryan, 1986). In the work of Hopfinger et al. (2004) it can be seen that this instability modifies the turbulent structure of the flow and substantially alters the sediment transport rate. Hopfinger et al. (2004) even reported the remarkable formation of sediment streaks due to the stresses generated by Görtler vortices.

The main objective of this research is to study the dynamics of Görtler vortices by carrying out DES simulations based on the experimental setup of Hopfinger et al. (2004) and Albayrak et al. (2008), for the turbulent flow in a scour-hole downstream of a sluice gate. The description of the flow and the experiences of Albayrak et al. (2008) are discussed in section 2. In section 3 we show the governing equations of the flow and describe the numerical model. Section 4 and 5 contain the principal results obtained from 3D simulations, comparing the results with the observations of Hopfinger et al. (2004) and Albayrak et al. (2008). The conclusions in section 6 summarize the results and outline future research.

2 FLOW DOWNSTREAM OF A SLUICE GATE

Hopfinger et al. (2004) and Albayrak et al. (2008) performed laboratory experiences of the flow downstream of a sluice gate. They studied the flowfield and the sediment erosion produced by Görtler vortices formed inside the scour hole. The experiments were conducted in a glass-side horizontal flume 17 m long, 0.5 m wide and 0.8 m deep (Albayrak et al., 2008). The hydraulic flume used in these experimental investigations is shown schematically in figure 1. A sluice gate was installed at the middle of channel, and at a short distance from the beginning of the sand bed (L_f = 0.1 m). The mobile bed was filled with uniformly graded sand of mean grain diameter d_{50} = 2 mm, which constitutes a hydraulically rough surface. The downstream water depth was kept constant at h_2 = 0.22 m by adjusting a gate at the downstream end of the flume and the upstream water depth h_1 was kept constant during the experiments by an overflow gate to produce a constant water discharge Q. The characteristic jet velocity, $U = \sqrt{2g\Delta h}$, where $\Delta h = h_1 - h_2$, with h_1 = 0.247 m. Using the downstream water depth as length-scale of the flow, the Reynolds number is equal to Re = 156,200. It is important to note that the drowned hydraulic jump produced downstream the sluice gate not alter the conditions of the free surface yielding a low Froude number in the scoured region.

Initially, the mobile bed was covered with a thin plate about 1 m long and the water levels were adjusted to the desired values. At time t = 0, this plate was suddenly withdrawn. After this reached in time $t = t_S$, a quasi-steady-state maximum scour depth $h_S = h_m$. In this investigation we perform the simulations at this state of advanced quasi-steady erosion, for which the scour hole has a significant curvature and Görtler vortices appear. The characteristic quasi-steady-state maximum scour depth is h_s = 0.064 m (Albayrak et al., 2008). These conditions produce a complicated situation to be modeled, due to the locally accelerated flow and the large scour-hole produced downstream of the gate as shown in figure 1. It is important to note that our simulations were conducted assuming that the bed is fixed, as sediment transport processes will be addressed in future research.

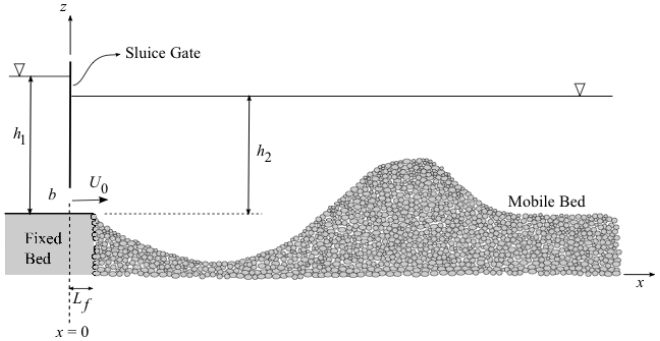

Figure 1. Schematic representation of the advanced scour conditions in the experiments carried out by Albayrak et al. (2008). Flow downstream of a sluice gate with an opening of b = 0.05 m, an apron of longitude L_f =0.1 m and a velocity scale equal to U_0 = 0.71 m s^{-1}.

3 NUMERICAL METHODS

To simulate the flow downstream of the sluice gate (Hopfinger et al., 2004; Albayrak et al., 2008), we solve the three-dimensional unsteady Reynolds-averaged Navier-Stokes equations (URANS) with a dual-time stepping artificial compressibility (AC) scheme (Paik et al., 2007). The system of governing equations is expressed as follows,

$$\frac{\partial u_i}{\partial x_i} = 0$$
$$\frac{\partial u_i}{\partial t} + u_j \frac{\partial u_i}{\partial x_j} = -\frac{\partial p}{\partial x_i} + \frac{1}{\mathrm{Re}} \frac{\partial^2 u_i}{\partial x_j \partial x_j} + \frac{\partial}{\partial x_j} \left\langle u_i' u_j' \right\rangle \quad (1)$$

where x_i are the Cartesian coordinates, u_i are the velocity components, p is the pressure plus the diagonal component of the Reynolds stress tensor, u_i' are the velocity fluctuations, and Re is the Reynolds number. The last term in the momentum equation represents the Reynolds stresses.

Since conventional URANS models to close Eq. (1) fail to capture the unsteadiness of coherent structures such as Görtler vortices, and full wall resolving LES might need large computational resources for practical Reynolds numbers, we employ the DES approach, which is a hybrid URANS/LES turbulence model (Spalart et al., 1997; Spalart, 2009). This model is based on turbulence proposed by Spalart and Allmaras (1994), which can be expressed as follows,

$$\frac{\partial \tilde{\nu}}{\partial t} + \frac{\partial}{\partial x_j}\left(u_j \tilde{\nu}\right) = \Gamma + \Theta + \Psi \quad (2)$$

where the working variable $\tilde{\nu}$ has a direct relation with the turbulent eddy-viscosity ν_t, Γ is the production term, Θ is the destruction term, and Ψ is the turbulent diffusion. In the hybrid DES approach developed by Spalart et al. (1997) the S-A turbulence model in Eq. (2) functions as the subgrid scale (SGS) model of LES in regions away from the wall, where the grid density can resolve the scales of fluid motion near the size of the grid spacing. For the rough-wall simulations performed in this investigation we also use the modification of the turbulence model proposed by Aupoix and Spalart (2003).

The system of equations is integrated in pseudo-time using a pressure-based implicit preconditioner enhanced with local time stepping and V-cycle multigrid acceleration in spanwise direction (Paik et al., 2007; Escauriaza and Sotiropoulos, 2010). The AC form of the governing equations is discretized using a second-order-accurate finite-volume method on a non-staggered computational grid. The domain is discretized using a boundary-fitted structured mesh to cluster efficiently the nodes in regions of interest, and adapt to the complex as shown in figure 2.

No-slip boundary conditions are applied to solid walls, and a rigid-lid assumption was employed at the free surface due to the low Froude numbers of the original experiments carried out by Albayrak et al. (2008).

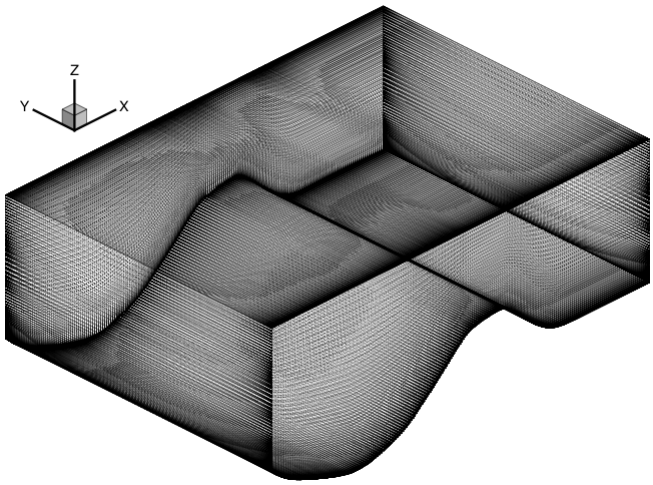

Figure 2. Three-dimensional layout of the scoured bed obtained from the experimental results of Albayrak et al. (2008). The computational domain has a total of 9.7 million grid nodes, with 209, 521 and 89 nodes in i, j and k-directions respectively. More than 50% of nodes are concentrated in the first 10% of water depth.

4 TURBULENT FLOW STRUCTURE IN THE SCOUR HOLE

The DES simulations are carried out in the scour hole region, assuming no-slip boundary conditions at solid walls. At the inlet we prescribe a converged URANS solution, previously computed in a separate calculation, which considers the entire length of the upstream rectangular channel and the geometry of the sluice gate. All the results presented in this investigation are obtained by using a non-dimensional physical time-step of t = 0.005. In this section we first show qualitatively the in-

stantaneous resolved flow in the scour hole and then we compute instantaneous variables to reproduce the experimental observations reported by Albayrak et al. (2008).

The results of our simulations demonstrate that our model can capture the coherent structures of flow, and in particular the Görtler vortices, as shown in figure 3. In this image we visualize the vortices by using the *q*-criterion (Hunt et al., 1988), which is calculated as follows,

$$q = \frac{1}{2}\left(\Omega_{ij}\Omega_{ij} - S_{ij}S_{ij}\right) \tag{3}$$

where Ω_{ij} represents the asymmetric part of the rate strain tensor and contain vorticity terms. S_{ij} represents the symmetric part of the rate strain tensor.

Theoretical and experimental studies identify the Görtler vortices as pairs of counter-rotating streamwise near-wall structures, which are shown in figure 3, where intense black and white colors represents negative and positive vorticity in streamwise direction. Figure 3 shows clearly that these vortices emerge downstream of the maximum depth inside the scour hole, coinciding with the qualitative observations of Hopfinger et al. (2004). As mentioned earlier these streamwise vortices are developed by the effects of the concave bed on the flow structure, triggering the boundary layer instability (Floryan, 1986). It is important to mention, these vortices appear without imposing an unsteady pseudo-turbulent inflow condition. The centrifugal instability is naturally excited by the resolved flowfield inside the scoured region.

Animations of the coherent structures visualized with *q*-isosurfaces show that inside the scoured region the flow is dominated by the shear-layer that emanates from the flat-bed channel and the wall-jet coming from the sluice gate. These vortices exhibit smaller time-scales compared to the Görtler vortices, which appear intermittently above the bed and seem to be dominated by lower-frequencies.

The emergence of counter-rotating vortices can also be studied by plotting countours of streamwise vorticity (Ω_X). In figure 4 (a) we can observe the Görtler vortices in the plane Y-Z at x/b = 0.7, inside the scour hole. The instantaneous streamlines and vorticity contours plotted in the zoomed area in figure 4(b), show that the flowfield is drastically altered in the concave region of the bed. After the boundary layer reattaches in the scour hole, highly unsteady vortices emerged and form mushroom-like structures with converging lateral flow, and strong vertical flow away from the wall, a feature of Görtler vortices that has commonly been observed as reported in the literature (Saric, 1994; Tandiono et al., 2008)

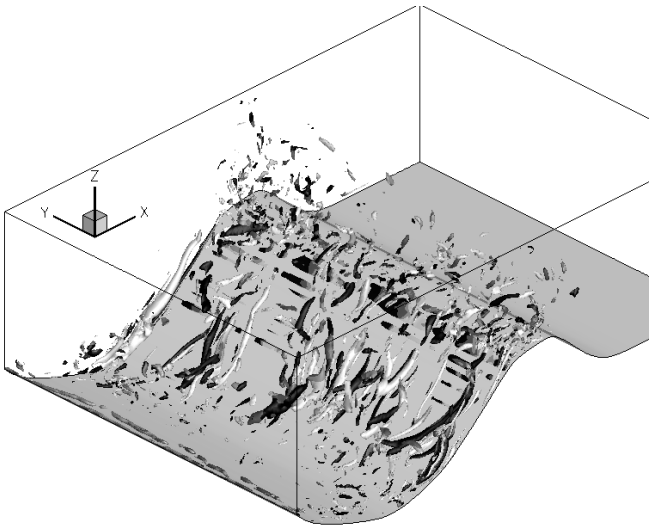

Figure 3. Instantaneous 3D vortical structures on the concave bed visualized with *q*-isosurfaces. In dark and bright colors are vortices with negative and positive vorticity in streamwise direction.

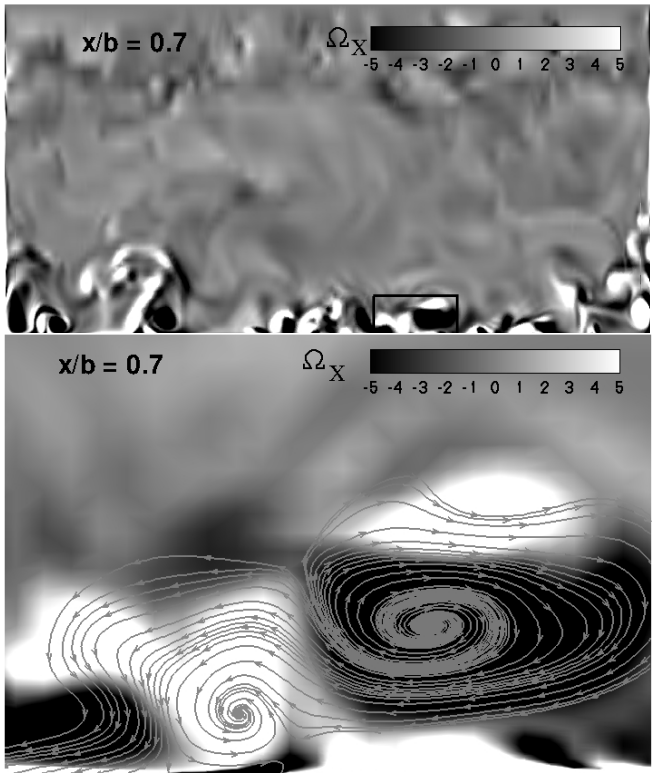

Figure 4. (a) Countours of vorticity in *x*-direction. (a) Non-dimensional streamwise vorticity contours in the entire plane. (b) Zoomed area inside the rectangle with instantaneous streamlines shows clearly the counter-rotating vorticity and the mushroom structure generated by the vortex pair.

Albayrak et al. (2008) reported the vertical magnitude of the Görtler vortices at the Y-Z plane for x/b = 0.7. They observed that the coherent streamwise structures had an approximate height of 3 cm. Vorticity contours in figure 5 depict an instantaneous image of the Görtler vortices at the same plane, showing that the vertical scale of the structures coincide with the experimental measurements.

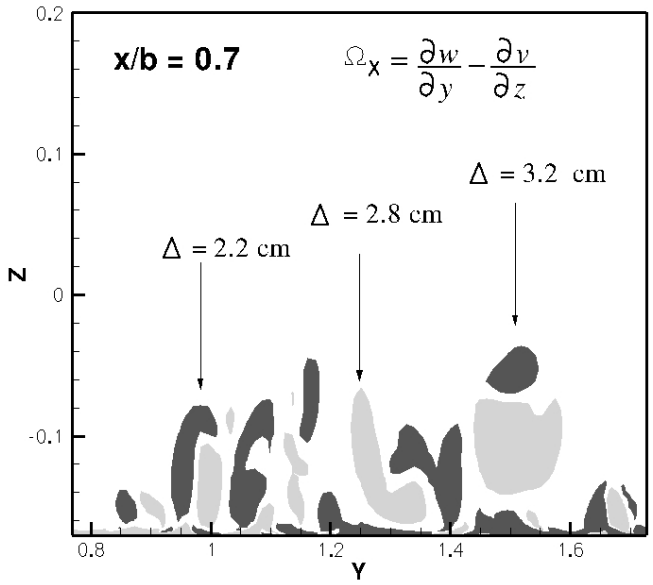

Figure 5. Contours of vorticity in *x*-direction at x/b = 0.7, according to the reference system defined in figure 1. In dark gray color is showed positive vorticity and in gray color negative vorticity. Magnitude of Görtler vortices that appear at center of the channel exhibit the same scales of the experiments.

5 SHEAR STRESS AND STATISTICAL FLOW RESULTS

Our simulations show the turbulent Görtler vortices that are formed in the downstream section of the concave bed. These vortices are dominated by low-frequency unsteadiness, and they are directly responsible for the increments on the instantaneous stresses on the bed. Figure 6 shows the instantaneous non-dimensional shear velocity (u_τ) at the bed. We can observe an increase in the intensity of u_τ in the zone where Görtler vortices are developed. Figure 7 shows the spatial variation of instantaneous non-dimensional shear velocity at the plane x/b = 0.7, along the spanwise direction across the Görtler vortices. When these vortices are present, the shear-stress has a seemingly periodic variation across the channel. This effect was reported by Hopfinger et al. (2004), as they observed considerable increments of sediment transport rates in this area of the bed.

High values of u_τ in figure 7 correspond to the positions of the streamwise vortices, while lower values are located in between them. This plot also has a remarkable similarity with the skin friction profiles reported in the recent experiments of Tandiono et al. (2009), who measured the effects of Görtler vortices in the turbulent flow inside a curved rectangular duct.

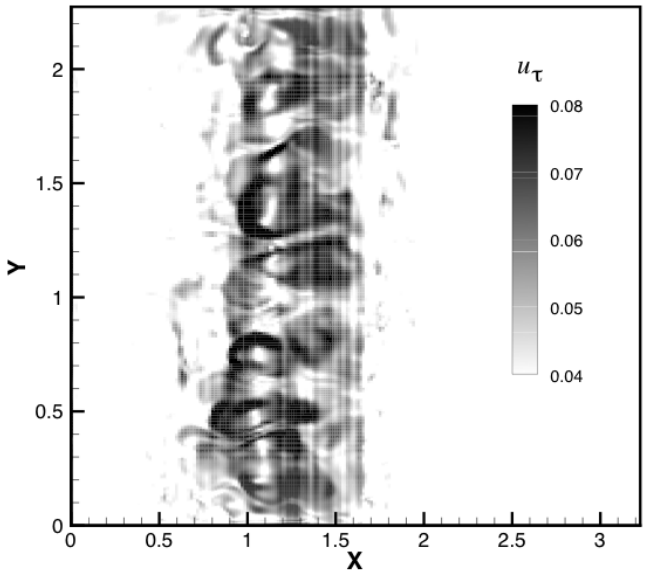

Figure 6. Instantaneous non-dimensional shear velocity at the bed. This is a significant increase on the shear-velocity magnitude where Görtler vortices are developed.

The spatial variation of shear-stress generated by the Görtler vortices is also responsible for the emergence of bed forms, identified as sediment streaks by Hopfinger et al. (2004). Their experimental visualizations showed the appearance of streamwise oriented streaks on the mobile bed, which were identified as evident signs of the presence of Görtler vortices and their effects on bed-load transport and scouring processes.

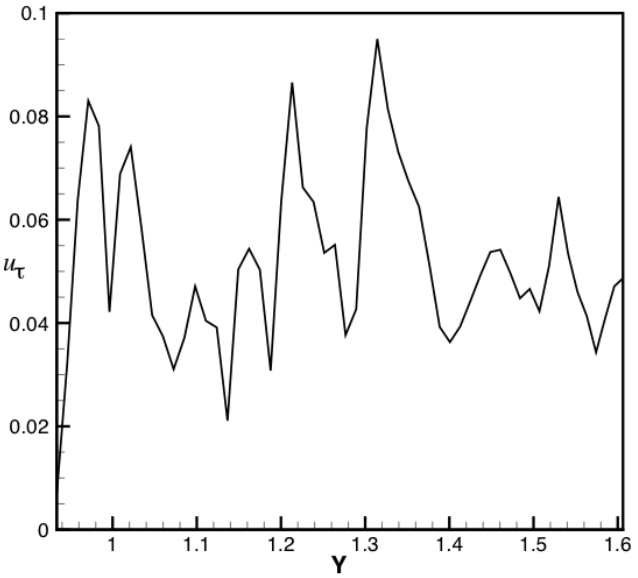

Figure 7. Visualization of instantaneous non-dimensional shear velocity (u_τ) at the bed. Variations of the shear-stress at plane x/b = 7 (system reference used by Albayrak et al. (2008), see figure 1) in the spanwise direction of the channel are associated with Görtler vortices.

In the streamwise direction we observe that the shear-velocity presents higher magnitudes in the section comprised by 7 < x/b < 9, at the center of the channel. This feature, attributed to the Görtler vortices and shown in figure 8, was also described in the experimental investigation of Albayrak et

al. (2008). With respect to this area of high stress, they make the following comment:

"This higher dimensionless friction velocity on the concave wall, when x/b > 7, can be attributed to the development of Görtler vortices. When x/b > 9, the friction velocity on the concave wall starts to decrease, because after that point the boundary slope changes and the Görtler vortices disappear."

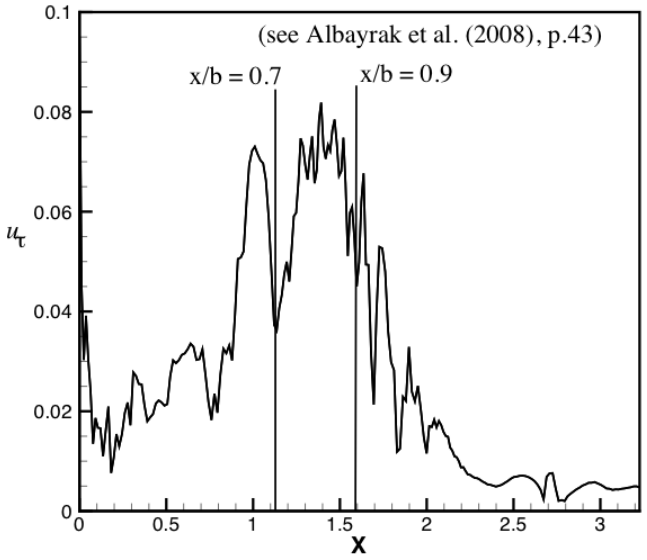

Figure 8. Visualization of instantaneous non-dimensional shear-velocity at the bed and at the center of channel. Variations of shear velocity in streamwise direction show an increase at the concave surface where Görtler vortices are developed.

From our simulations we can reproduce additional quantitative results that were also obtained by Albayrak et al. (2008). Employing instantaneous measurements of the velocity field in a vertical profile, they compute the product of horizontal and vertical velocity fluctuations in time, capturing upwash and downwash flow events near the bed.

These events are characterized by positive and negative values of the instantaneous components of the Reynolds stress tensor. Along a vertical line in the center of the channel, at a position x/b = 0.7, the flowfield is plotted in time. The vertical distance is non-dimensionalized by using the length scale $z'_{1/2}$, defined as the height at which the velocity magnitude is equal to half of the maximum streamwise velocity.

Remarkably, the simulations presented in this research can capture the same dynamics described by Albayrak et al. (2008). In figure 9 (a) we plot the velocity components and contours of *u'w'* in time, using the resolved flowfield from the DES calculation. This figure shows the predominant contribution of upwash events on the Reynolds stresses. In the outer layer, the downwash and upwash flow events are dominant at several locations, see for example $z'/z'_{1/2}$ =1 and $z'/z'_{1/2}$ =0.5 at t=8.9 s and t=9.2 s.

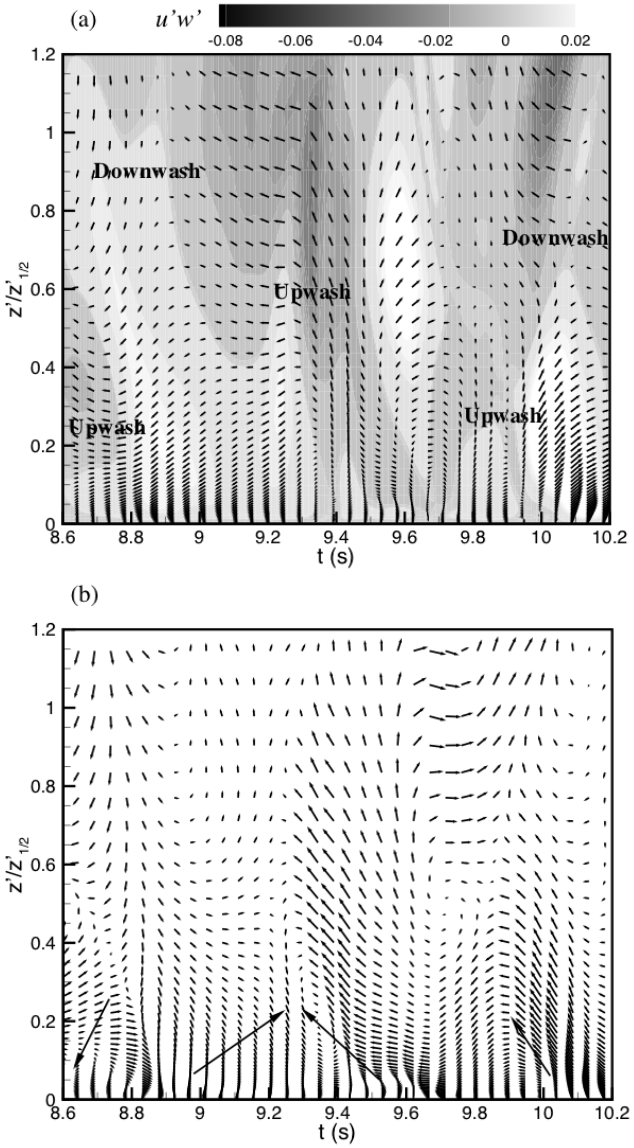

Figure 9. Two-dimensional resolved velocity vector plots along a vertical profile at plane x/b=0.7, at the center of the channel. The total time interval is Δt=1.6 s. The length scale is $z_{1/2}$ = 5.8 cm on the selected profile. (a) Streamwise (*x, z'*)-plane, velocity vectors *u'*, *w'*; (b) Spanwise (*y, z'*)-plane, velocity vectors *v'*, *w'*.

The same statistical observations were made by Albayrak et al. (2008) (see p. 41), who linked these dynamic processes to the unsteadiness of the near-wall coherent vortices. Convergent flow observed in plots of *v'-w'* velocity vectors which were reported by Albayrak et al. (2008), are also reproduced in our simulations as shown in figure 9 (b).

Another quantitative result that has a direct relation with the influence of Görtler vortices on sediment transport rates in the scoured region is the Reynolds stress obtained from the resolved velocity fluctuations. Figure 10 shows the <uw> Reynolds stress computed by Albayrak et al. (2008) at plane x/b=0.6 and the results obtained with our simulations. In this figure is clear that

DES represent with a good accuracy the experimental results measured by Albayrak et al. (2008).

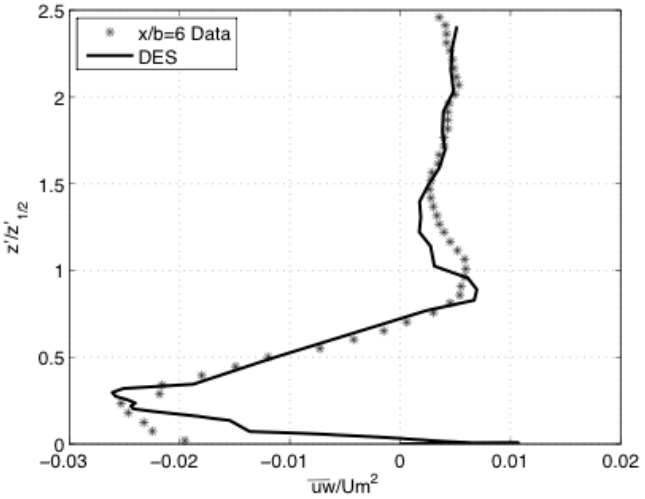

Figure 10. Normal Reynolds stress computed in experiments made by Albayrak et al. (2008) and the DES model. The values of Reynolds stress are scaled by U_m, which correspond to the maximum streamwise average velocity.

6 CONCLUSIONS

In this investigation we perform numerical simulations of the flow downstream a submerged sluice gate over a rough concave bed at Re=156,200. We reproduce the configuration of the scour experiments carried out by Albayrak et al. (2008).

The flow is characterized by a wide range of time and length scales, dominated by unsteady coherent structures induced by the complex geometry of the domain and the wall-jet coming from the sluice gate. The resolved flowfield computed from DES simulations shows that our model successfully captures the dynamic features of the coherent structures within the scour hole, and the formation of Görtler vortices near the bed. Pairs of highly unsteady counter-rotating streamwise vortices appear inside the scoured region, forming mushroom-like structures that have been reported in multiple studies of turbulent boundary layer flows over concave surfaces.

We also reproduce quantitative experimental results reported by Hopfinger et al. (2004) and Albayrak et al. (2008). Plots of instantaneous shear velocity at the bed show that Görtler vortices are directly responsible for the increase of bed stresses, and consequently for the larger sediment transport rates that were observed by Hopfinger et al. (2004). The simulations capture statistically the same upwash and downwash flow events reported by Albayrak et al. (2008) with similar time-scales, including the increments of instantaneous Reynolds stresses obtained from resolved velocity fluctuations. The model captured in detail the dynamics of the Görtler vortices in this complex flow. This information is critical to employ new methods to determine bed-load transport and scour induced by turbulent coherent structures. This work will be carried out in future research.

REFERENCES

Albayrak, I., Hopfinger, E. J. & Lemmin, U. 2008. Near-field flow structure of a confined wall jet on lat and concave rough walls. *J. Fluid Mech.*, 520, 27-49.

Aupoix, B. & Spalart, P. R. 2003. Extensions of the Spalart-Allmaras turbulence model to account for wall roughness. *Int. J. Heat Fluid Flow* , 24, 454-462.

Escauriaza, C. & Sotiropoulos, F. 2010. Reynolds numbereffects on the coherent structures dynamics of the turbulent horseshoe vortex system. *accepted in Flow Turbul. Combust* .

Floryan, J.M. 1986. Görtler instability of boundary layers over concave and convex walls. Phys. Fluids , 29, 2380-2387.

Hopfinger, E.J., Kurniawan, A., Graf, W.H. & Lemmin, U. 2004. Sediment erosion by Görtler vortices: The scour-hole problem. *J. Fluid Mech.*, 520, 327-342.

Hunt, J. C. R., Wray, A. A. & Moin, P. 1988. Eddies, stream and convergence zones in turbulent flows. *Proc. of the Summer Program,* Center for Turbulence Research, NASA Ames/Stanford Univ., pages 193-208.

Paik, J., Escauriaza, C. & Sotiropoulos, F. 2007. On the bimodal dynamics of the turbulent horseshoe vortex system in a wing-body junction. *Phys. Fluids*, 19, 045107.

Saric, W. 1994. Görtler vortices. *Annu. Rev. Fluid Mech.*, 26, 379-409.

Spalart, P.R. 2009. Detached-eddy simulations. *Annu. Rev. Fluid Mech.*, 41, 181-202.

Spalart, P. R. & Allmaras, S. R. 1994. A one-equation turbulence model for aerodynamic flows. *Rech. Aerosp.*, 1, 5-21.

Spalart, P. R., Jou, W. H., Strelets, M. & Allmaras, S. R. 1997. Comments on the feasibility of LES for wings and on a hybrid RANS/LES approach. *Advices in DNS/LES*, C. Liu and Z. Liu, eds., Greyden Press, Columbus OH.

Tandiono, Winoto, S. H. & Shah, D. A. 2008. On the linear and nonlinear development of Görtler vortices. *Phys. Fluids*, 20, 094103.

Tandiono, Winoto, S. H. & Shah, D. A. 2009. Wall shear stress in Görtler vortex boundary layer flow. *Phys. Fluids*, 21, 084106